Frontiers in Health Informatics
2023; 12: 153
www.ijmi.ir
Open Access

Electronic and structural properties of core-shell amino-silica nanoparticles: DFT and SCC-DFTB calculation

Fatemeh Houshmand[1]*, Jeremy Schofield[2], Zahra Moafi[1]

[1]Department of Industrial Chemistry Engineering, Technical and Vocational University (TVU), Tehran, Iran
[2]Chemical Physics Theory Group, Department of Chemistry, University of Toronto, Toronto, Ontario, Canada

Article Info

Article type:
Research

Article History:
Received: 2023-07-24
Accepted: 2023-08-07
Published: 2023-08-16

**** Corresponding author:***
Fatemeh Houshmand

Department of Industrial Chemistry Engineering, Technical and Vocational University (TVU), Tehran, Iran

Email: fhoushmand@tvu.ac.ir

Keywords:
Amino Decorated Silica Nanoparticles
Silicon Dioxide Clusters
Electronic Band Structure
Density of States

A B S T R A C T

Introduction: Silica nanoparticles (SNP) are extremely promising tools in nanotechnology and nano medicine. In most of applications such as capture and release of bacteriophage viruses the nano-structures of silica are coated by bio-compatible groups such as amine compounds. The presence of amino groups on the surface of the biosensors enables the installation of analyte receptors and antifouling agents such as oligo (ethylene oxide). Therefore, in this study, the electronic and structural properties of Core-Shell amino-Silica Nanoparticles are investigated.

Material and Methods: In this investigation, we aim at obtaining the optimized structures and evaluate the geometries of the ground state for (SiO_2) n (n=16, 20) nanoclusters. The electronic properties computed by density functional theory with GGA approximation and SCC-DFTB with hybrid Slater-Koster files are investigated and the effect of functionalization on such properties is discussed.

Results: Solvolysis of studied structures is examined and it is shown that the highest occupied and lowest unoccupied molecular orbital states shift to obviously higher energy levels, which lead to more stable hydrogenated nanoclusters. The stability of nanoclusters rises by functionalization with amino and methylamine groups. Charge analysis of functionalized systems indicates the reactivity of nanoclusters. The results obtained in this paper are useful for chemical and biochemical applications of silica nanostructures.

Conclusion: Results show that the length of amine hydrocarbon chain can control the electronic and magnetic properties of studied silica nanocluster (SNP) with different number of SiO_2 unit. Pure ultra-small nanocluster shows the impressive spin splitting around the Fermi level, which is due to the spin splitting of outer silicon atoms. This feature of silica nanoclusters may be notable for applications in electronics.

Cite this paper as:
Houshmand F, Schofield J, Moafi Z. Electronic and structural properties of core-shell amino-silica nanoparticles: DFT and SCC-DFTB calculation. Front Health Inform. 2023; 12: 153. DOI: 10.30699/fhi.v12i0.481

INTRODUCTION

Silica is an important material with outstanding properties in various areas of scientific and engineering interest. In the past decades, significant progress has been made to investigate various properties of silica nanoparticles. Recently, low-dimensional silica has attracted much attention in experimental [1] and computational studies [2], because of the potential applications in electronics, optics [3], diagnostic sensors and biosensors [4, 5], chemical nanodevices and theragnostic agent [6] and in therapeutic drug delivery and nanomedicine [7-9].

Comparing to bulk silica, highly stable nano-sized silica has a number of novel properties including light adsorption, ion exchange, and light emitting [4, 10-12].

Most of the properties of silica nanoclusters can be provoked using proper functionalization. For instance, in nano-medicine, functionalized silica nanoparticles have been used for plasma DNA transport [13], capture and release of bacteriophage viruses [14] and synthesis of silica-polypeptide composite particles [15]. In most of these applications, biocompatible groups such as amine compounds coat the nano-structures of silica. The

presence of amino groups on the surface of the biosensors enables the installation of analyte receptors and antifouling agents such as oligo (ethylene oxide) [16]. Most of these properties of silica nanostructures can be related to the combination of their orbitals. It has been found that not only the 3s and 3p orbitals but also the 3d orbitals of silicon contribute to the formation of the top of the valence band of SiO_2 [17].

The structure of SiO_2 clusters in different size` has been intensively investigated experimentally and theoretically [18-29]. Nonetheless, some features of the electronic structure of SiO_2 remain unclear. Extensive efforts have been devoted to determining the stable structures and investigate various properties of silica nanoparticles with ultra-small structures .The literatures have explored the properties of isomers of small stoichiometric silica clusters by using one of these methods; density functional theory (DFT) minimization energy using bulk-parametrized interatomic potentials , using repeated subunits with structures energy-minimized using DFT, annealing of bulk silica fragments using classical molecular dynamics with bulk-parametrized interatomic potentials, followed by DFT energy minimization or ,in some of investigations , combining interatomic potentials with the Basin Hopping (BH) global optimization algorithm to search for low-lying minima on the silica nanocluster energy landscape [18, 19].

In the present research, we want to evaluate the optimized geometrical structures of the ground state of (SiO_2) n (n=16, 20) clusters, functionalized with amine and amino groups. In addition, the electronic properties of these structures are investigated in detail.

MATERIAL AND METHODS

DFT calculations were carried out using plane-wave basis set and ultra-soft pseudo-potentials as implemented in the QUANTUM ESPRESSO package [30]. The generalized-gradient approximation (GGA) with the Perdew-Burke-Ernzerhof (PBE) functional [31] and a cutoff of 600 eV for the plane-wave basis set were used in all computations.

Two different sizes of silicon dioxide (SiO_2) nanoclusters with n=16 and 20 were considered as q1 and q2 models, respectively (Fig 1). Their structures are optimized through variable cell-shape relaxation method by damped (Beeman) dynamics of the Parrinello-Rahman extended lagrangian are obtained and then energy minimization done by DFT method. The geometries of the nano-clusters with and without adsorbed species were optimized using the gamma point, with convergence thresholds of 1×10^{-5} eV in energy and 0.001 eV/Å in force. A 3×3×3 grid of k-points generated by Monkhorst-Pack [32] scheme was used to calculate energy and other properties.

Self-consistence charge density functional tight binding implemented in DFTB+ package [33] is performed for calculating the density of states. The pbc-0-3 parameter sets are considered for Slater-Koster files. The pbc set is developed with a focus on solid state systems. All parameters for solving Hamiltonian are used as same as DFT calculations.

A cubic super cell with the edge length of 21.33 Å was used and repeated periodically along x, y and z directions, which had a vacuum region of 10 Å was applied in all directions to exclude the mirror interactions between adjacent images.

In order to compare the electronic properties of nanostructures with those of a single layer of silica, a (0, 0, 0, 1) surface of silica was selected. The dimensions of hexagonal supercell of silica were a=b=9.83 Å and c=20 Å.

RESULTS

Structural parameters for the optimized q1 and q2 nanoclusters are shown in Fig 1. As can be seen, upon optimization, q1 loses the structural symmetry and forms a twisted shape. In q2 on the other hand, three SiO4 tetrahedra form a closed triangle, which is the basic structural unit of quartz. The cohesive energy for these structures is evaluated from

$$E_{coh} = E[(SiO_2)_n] - n\,E[Si] - 2n\,E[O] \qquad (1)$$

where $E[(SiO_2)_n]$, E[Si] and E[O] are the total energies of the nanocluster and isolated silicon and oxygen atoms in a same supercell, respectively. Table 1 contains the cohesive energies per atom for q1 and q_2. The cohesive energy is lower for q_2, which means that q2 is more stable than q1.

The density of states (DOS) plots is shown for q1 and q2 structures. The computed DOS data are in good agreement with previous studies [34]. As can be seen, DOS for q1 shows different spin-up and spin-down densities, while q2 has almost similar characteristics for up and down states. This is more obvious near the Fermi level. For q2, there is a strong spin-up peak below the Fermi level and a similar spin-down peak above it. Fig 2 illustrates the highest occupied and lowest unoccupied molecular orbitals (HOMO and LUMO) for q2. The LUMO state is mainly spin-down, while the HOMO is mainly spin-up.

Table 1: Magnetic moment (μ), total force (Ftot), binding energy (Eb), Fermi energy (Ef) from DFT (from DFTB+) and charge transfer (ΔQ) for bare and functionalized nanoclusters

system	μ(bohr/cell)	*F*tot (Ry/au)	E_b (eV/atom)	E_f (eV)	ΔQ_{Si} (e)	ΔQ_O (e)	ΔQ_H (e)	ΔQ_N (e)
q1	14.82	2.615	−5.573*	−7.53	0.147	−0.214		
q1H	0.77	0.740	−5.990	−5.59	−0.238	0.345	0.238	0.238
q2	20.57	0.066	−6.158*	−6.83	0.213	−0.176		
q2–NH_2	19.96	2.775	+5.321	−6.67	−0.116	0.153		0.116
q2H	−0.29	0.024	−7.670	−4.35	−0.015	0.338	0.015	0.015
q2H–NH_2	−0.20 (-0.32)	0.957(0.95)	-7.87	−4.33(-5.54)	−0.105	0.023	0.154	0.105
q2H–CH_2NH_2	0.24 (-0.42)	1.159(0.95)	−6.734	−4.58(-5.54)	0.107	−0.008	0.065	−0.107
q2H–$C_2H_4NH_2$	0.24 (-0.35)	1.223(0.95)	−6.806	−4.44(-5.54)	0.102	−0.003	0.069	−0.102
q2H–$C_3H_6NH_2$	0.01 (-0.55)	1.264(0.95)	−6.810	−2.82(-5.54)	0.122	−0.109	0.069	−0.122

* Cohesive energy per atom form (1).

The spin splitting near the Fermi level means different spin-up and spin-down transmissions along the structure in low bias voltages. Such splitting and different transmissions are favorable as fundamental characteristics in spintronics. Despite different values of band gaps, both nanoclusters are semiconductor. However, bulk silicon dioxide is an insulator. This feature has been already observed in metal oxide clusters [35]. In the calculated DOS for bulk silica by DFT the peak in the top of the valence band is not present [36].

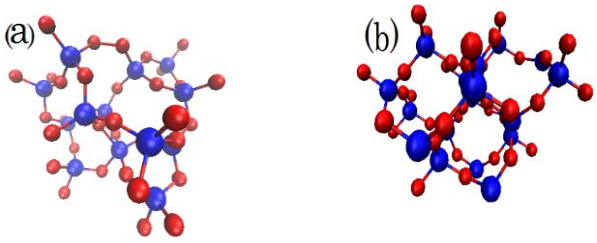

Fig 1: Optimized structures of (a) q1 (b) q2 . The silicon and oxygen atoms are shown in blue and red, respectively

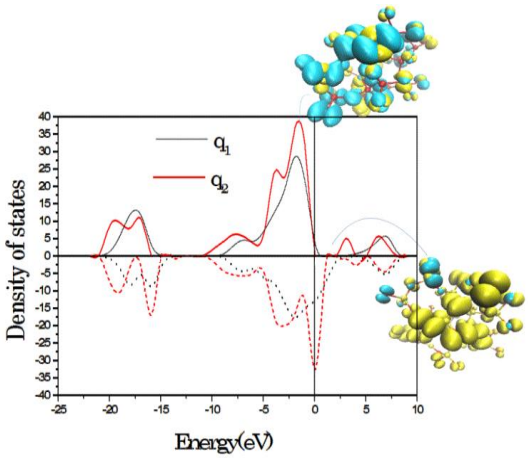

Fig 2: Density of states for q1 and q2. Spin-polarized charge density plots for HOMO (up) and LUMO (bottom) are also shown for q2 for an isodensity value of 2×10−4 μB/bohr3. Cyan (dark) and yellow (light) regions correspond to positive and negative polarization, respectively. Fermi level of energy is set to zero and dashed lines are for minority spin states

Fig 3 shows the spin-up and spin-down projected DOS (PDOS) plots of q2 along the z direction in different energies. In both plots, three main areas exist between 0.15 and 0.3 Å (place of outer atoms). These areas show that the main part of spin characteristics is due to the outer silicon atoms and are near the Fermi level, and about the energies of −0.25 and −0.75 eV. Despite edge Si atoms, inner Si atoms and oxygen atoms have not a major role in the DOS.

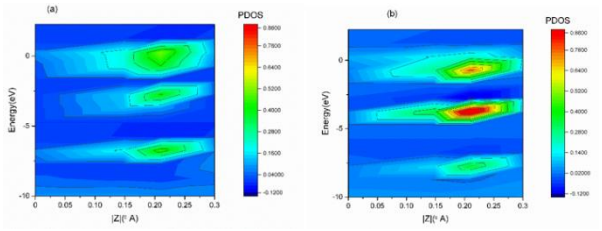

Fig 3: The DOS projected onto the Si atoms along the z direction for (a) majority spin and (b) minority spin states of q2

Fig 4 illustrates the effect of solvolysis on DOS of bulk surface silica and q1 and q2 nanoclusters. In solvent, because of high activity of the dendrite oxygen atoms, these atoms have a high tendency to bond to hydrogen. In fact, oxygen atoms are replaced by hydroxyl groups. Here, for ease of use, we denote fully hydroxyl terminated nanoclusters as qH. The hydroxyl terminated surface may change the electronic and magnetic properties of nanoclusters. Here, a sharp drop in the value of magnetization is observed and the DOS spectrum shifts to lower energies. This shift is larger for q2 than for q1. Moreover, the addition of hydrogen atoms to pristine silicon dioxide nanoclusters can convert them from p-type to n-type semiconductors.

The electron distribution of hydrogenated and bare q2 structures are illustrated in Fig 5. The electrons are localized on oxygen atoms. This confirms that these atoms are favorable sites for electron-accepting functional groups. In fact, the electron-donating functional groups such as amino groups attract to silicon atoms and cause stress in nanoclusters.

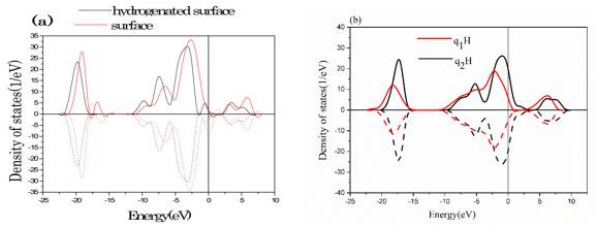

Fig 4: Density of states for bare and hydrogenated nanosurface (a) and hydrogenated nanoclusters (b)

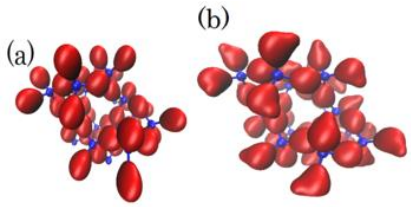

Fig 5: Diagrams of charge density for q2 and q2–H for an isodensity value of 0.1 e

After the evaluation of the active bonding sites for amine group, the next step was to find the activation energy along that path, so that kinetics of the recombination reaction could be forcasted. An initial path was constructed and represented by a discrete set of images of the system connecting the initial and final states. To calculate the activation energy barrier the nudged elastic band (NEB) method implemented in the Quantum ESPRESSO package is used. Results of activation energy for reaction between q2H and water molecule indicates that are suitable process. Functionalization of silica nano-cluster in an exothermic reaction occurs where a water molecule is released (Fig 6).

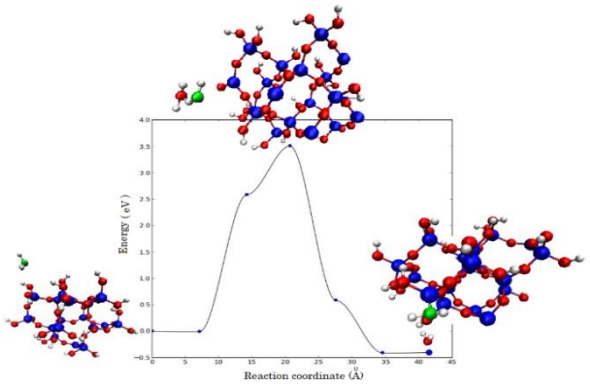

Fig 6: Calculated energy profile involved in the adsorption of NH2- on q2H. The optimized structures of initial, excited state and final images along the energy path are plotted in the inset

Based on a previous work, the most favorable situation is to replace one of the edge oxygen atoms by amino groups [37]. Fig 7 shows the optimized structures for amine group functionalization of q2.

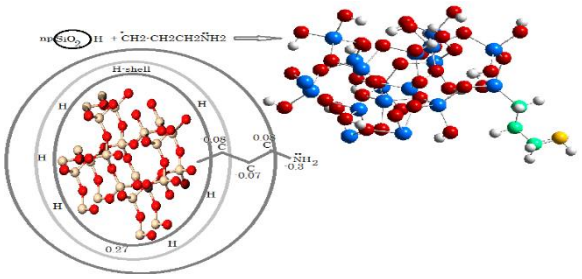

Fig 7: Schematic of functionalized q2. Number reflect the net value of charge for each atoms

As can be seen, these functional groups can deform the cluster structure. Recently, the amino-functionalized silica nanoparticles have been successfully fabricated [38]. In this work, the amino functional groups are added to the nanocluster along the (0, 0, 1) surface.

All terminated O-H groups have a potential to replacing by amino groups and making silica core-shell. Core–shell particles with different ranges of pore sizes in the shell are used in many applications such as chromatography and drug delivery. The productivity of manufacturing core–shell silica particles is low because high tendency of silica fragments to aggregation. Silica spheres are employed to prepare various inorganic/composite core–shell structures although silica can also be removed by acid etching or alkaline washing to produce hollow structures. Core–shell silica particles further coated with a layer of carbon because carbon is chemically inert and highly stable. Therefore, coating silica nano particle by carbon shell is desirable. According to results of this investigation, silica nano structure functionalized with amide chain due to homogenous charge density around amide chain can be stable. In next step, the core-shell particle of silica nano structure coated with amide shell is investigated. In next we investigate the stable structure of core silica nanostructure coated by amine rings.

DISCUSSION

Table 1 shows the binding energies for the functionalized q2 clusters. Functionalization of q2 with amino group is an endothermic process. In addition, as data shows, the amino group has no significant effect on magnetic moments of pristine and hydrogenated nanoclusters.

On the other hand, as Table 1 shows, the functionalized nanoclusters with amine groups are energetically more stable than the pristine ones. In addition, these processes are exothermic and the stability of the system increases by increasing the number of carbon atoms in the hydrocarbon chain of amine. Amine-group functionalization causes charge transfer from Si to amine group. In fact, the resonance

electron affinity of nitrogen atom overcomes the electronegativity. Because of that, electron density on nitrogen atom becomes higher and the reactivity of nanocluster for binding to other groups increases. However, in biosystems, the free electron pair on nitrogen can covalently bind to other electron acceptors and form a strong chemical bond. These strong bonds can affect or even damage the structure of the group which is bonded to the N atom. Therefore, in these applications, such as in drug delivery, a modest bond is more favorable [7, 8] and the amine groups connect to silica nanocluster via a hydrocarbon link. According to the value of charge transfer between N and Si atoms for q2H–CH2NH2 (Table 1) the presence of a hydrocarbon interface between amino group and silica nanostructure causes a balanced electron distribution on N–C bond at the interface.

The projected density of states plots for q2H-amine systems are shown in Fig 8 to 11.

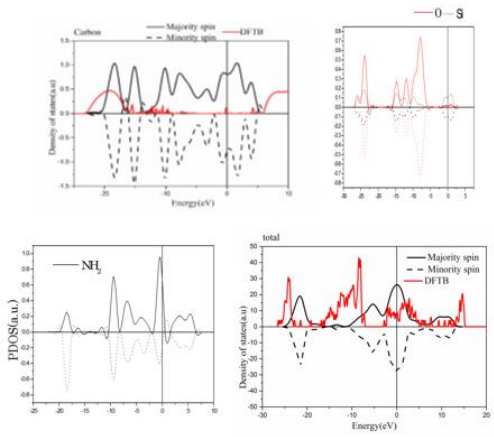

Fig 8: Projected density of states for q2H–C3H6NH2. In each part, the panels from up to down are total DOS, and PDOS for hydrocarbon chain, amino group and nearest neighbor Si and O atoms

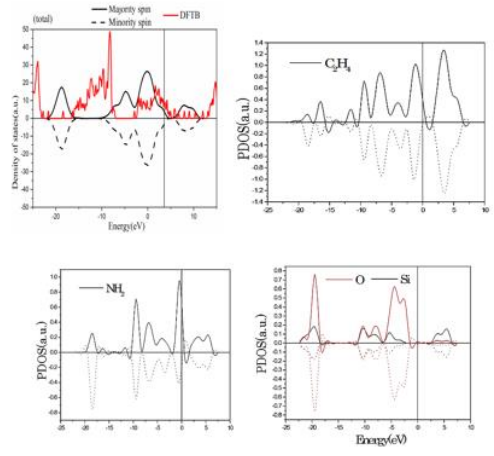

Fig 9: Projected density of states for q2H–C2H4NH2. In each part, the panels from up to down are total DOS, and PDOS for hydrocarbon chain, amino group and nearest neighbor Si and O atoms

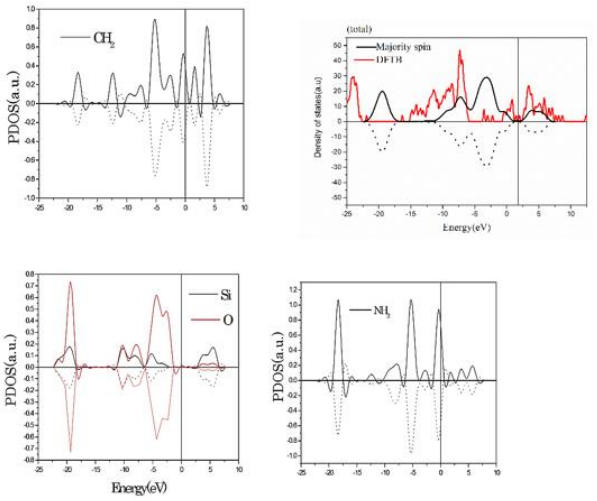

Fig 10: Projected density of states for q2H–CH2NH2. In each part, the panels from up to down are total DOS, and PDOS for hydrocarbon chain, amino group and nearest neighbor Si and O atoms

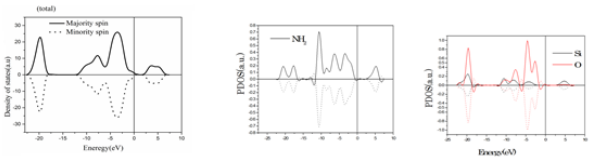

Fig 11: Projected density of states for q2H–NH2. In each part, the panels from up to down are total DOS, and PDOS for hydrocarbon chain, amino group and nearest neighbor Si and O atoms

By increasing the length of the amine hydrocarbon chain, the occupation of energy states near the Fermi level gradually becomes less. PDOS results show that this effect is due to amine group. It seems that in amine-functionalized silica nanoparticles the distance of functional group from silicone atoms affects the occupation of energy states of nanocluster.

Density functional theory and self-consistence charge density functional tight bonding are employed for calculating density of sates. According to Fig 8, results of these two methods are dramatically different. As density of states for carbon atoms shows, the main source of such difference is in calculating the energy occupation for carbon atoms. This nonconformity determines that generalized gradient approximation in interpretation of orbitals combination is weak. In self-consistence charge density functional tight bonding method, the hybrid Slater-Koster files are employed. Results of SCC-DFTB reflects that density functional theory and self-consistence charge density functional tight bonding calculate the occupation of each state of this nano-cluster totally different.

CONCLUSION

In this theoretical study spin-polarized DFT calculations with GGA approximation and also SCC-DFTB with hybrid Slater-Koster files have been used

to investigate the electronic and structural properties of functionalized silica nanoclusters. Findings show that silica nanoclusters with amine group are more stable whereas amino group causes instability in silica nano-structures. In addition, it is shown that the electronic and magnetic properties of studied silica nanocluster (SNP) with different number of SiO2 unit can be controlled by the length of amine hydrocarbon chain. This can be shown in future studies by investigating the electronic and magnetic properties of silica nanoclusters coated by amine chains on any active sits of silica nanocluster. Pure nanocluster shows the impressive spin splitting around the Fermi level which is due to the spin splitting of outer silicon atoms. This feature of silica nanoclusters may be notable for applications in electronics.

ACKNOWLEDGMENT

This research was enabled in part by support provided by WestGrid (www.westgrid.ca) and Compute Canada Calcul Canada (www.computecanada.ca).

AUTHOR'S CONTRIBUTION

FH: Conception and design of the study analysis and interpretation of data, Drafting the manuscript and revising the manuscript; ZM: Interpretation of data and revising the manuscript. JS: Running the computational calculations, analysis, and interpretation of data.

All authors contributed to the study's conception and design.

CONFLICTS OF INTEREST

The authors declare no conflicts of interest regarding the publication of this study.

FINANCIAL DISCLOSURE

The authors would like to appreciate the Technical and vocational university for supporting this research financially.

ETHICS APPROVAL

This research is a theoretical study supported by Technical and vocational university. All the data gathered by computational studies by Quantum espresso package and DFTB+ package.

REFERENCES

1. Al-Ruqeishi MS, Nor RM, Amin YM, Al-Azri K. Direct growth and photoluminescence of SiOx nanowires and aligned nanocakes by simple carbothermal evaporation. Silicon. 2011; 3(3): 145-51.
2. Jiang DE, Carter EA. First-principles study of the interfacial adhesion between SiO_2 and $MoSi_2$. Physical Review B. 2005; 72(16): 165410.
3. Chang EK, Rohlfing M, Louie SG. Excitons and optical properties of α-quartz. Phys Rev Lett. 2000; 85(12): 2613-6. PMID: 10978120 DOI: 10.1103/PhysRevLett.85.2613 [PubMed]
4. Cetin AE, Coskun AF, Galarreta BC, Huang M, Herman D, Ozcan A, et al. Handheld high-throughput plasmonic biosensor using computational on-chip imaging. Light: Science & Applications. 2014; 3(1): e122.
5. Zinoviev K, Carrascosa LG, del Río JS, Sepúlveda B, Domínguez C, Lechuga LM. Silicon photonic biosensors for lab-on-a-chip applications. Advances in Optical Technologies. 2008; 2008: 383927.
6. Wu Z, Sun DW, Pu H, Wei Q. A dual signal-on biosensor based on dual-gated locked mesoporous silica nanoparticles for the detection of Aflatoxin B1. Talanta. 2023; 253: 124027.
7. Piao Y, Burns A, Kim J, Wiesner U, Hyeon T. Designed fabrication of silica-based nanostructured particle systems for nanomedicine applications. Advanced Functional Materials. 2008; 18: 3745-58.
8. Chang JH, Kim KJ, Shin YK. Sustained drug release on temperature-responsive polymer hybrid nanoporous silica composites. Bulletin of the Korean Chemical Society. 2004; 25(8): 1257-60.
9. Li LL, Yin Q, Cheng J, Lu Y. Polyvalent mesoporous silica nanoparticle-aptamer bioconjugates target breast cancer cells. Advanced Healthcare Materials. 2012; 1(5): 567-72.
10. Marshall KE, Robinson EW, Hengel SM, Paša-Tolić L, Roesijadi G. FRET imaging of diatoms expressing a biosilica-localized ribose sensor. PLoS One. 2012; 7(3): e33771. PMID: 22470473 DOI: 10.1371/journal.pone.0033771 [PubMed]
11. Ning N, Calvo F, Van Duin ACT, Wales DJ, Vach H. Spontaneous self-assembly of silica nanocages into inorganic framework materials. The Journal of Physical Chemistry C. 2009; 113(2): 518-23.
12. Landers J, Gor GY, Neimark AV. Density functional theory methods for characterization of porous materials. Colloids and Surfaces A: Physicochemical and Engineering Aspects. 2013; 437: 3-32.
13. Wei H, Wang E. Nanomaterials with enzyme-like characteristics (nanozymes): Next-generation artificial enzymes. Chemical Society Reviews. 2013; 42(14): 6060-93.
14. Cheang TY, Tang B, Xu AW, Chang GQ, Hu ZJ, He WL, et al. Promising plasmid DNA vector based on APTES-modified silica nanoparticles. Int J Nanomedicine. 2012; 7: 1061-7. PMID: 22403488 DOI: 10.2147/IJN.S28267 [PubMed]
15. Rosu C, Selcuk S, Soto-Cantu E, Russo PS. Progress in silica polypeptide composite colloidal hybrids: From silica cores to fuzzy shells. Colloid and Polymer

Science. 2014; 292(5): 1009-40.

16. Fong B, Russo PS. Organophilic colloidal particles with a synthetic polypeptide coating. Langmuir. 1999; 15(13): 4421-6.

17. Yamanaka T, Mimaki J, Tsuchiya T. The bond character of rutile type SiO2, GeO2, and SnO2 was investigated by molecular orbital calculation. Zeitschrift für Kristallographie - Crystalline Materials. 2000; 215: 419-23.

18. Flikkema E, Bromley ST. Dedicated global optimization search for ground state silica nanoclusters: (SiO2) N (N=6– 12). The Journal of Physical Chemistry B. 2004; 108(28): 9638-45.

19. Harkless JA, Stillinger DK, Stillinger FH. Structures and energies of SiO2 clusters. The Journal of Physical Chemistry. 1996; 100(4): 1098-1103.

20. Kong Q, Zhao L, Wang W, Wang C, Xu C, Zhang W, et al. Magic number silicon dioxide-based clusters: Laser ablation-mass spectrometric and density functional theory studies. J Comput Chem. 2005; 26(6): 584-98. PMID: 15739194 DOI: 10.1002/jcc.20194 [PubMed]

21. Ding YC, Chen M, Gao XY, Jiang MH. Theoretical investigation on the electronic structure, elastic properties, and intrinsic hardness of Si2N2O. Chinese Physics B. 2012; 21(6): 067101.

22. Du J, Corrales LR, Tsemekhman K, Bylaska EJ. Electron, hole and exciton self-trapping in germanium doped silica glass from DFT calculations with self-interaction correction. Nuclear Instruments and Methods in Physics Research Section B: Beam Interactions with Materials and Atoms. 2007; 255(1): 188-94.

23. Bromley ST, Flikkema E. Columnar-to-disk structural transition in nanoscale (SiO2) N clusters. Phys Rev Lett. 2005; 95(18): 185505. PMID: 16383916 DOI: 10.1103/PhysRevLett.95.185505 [PubMed]

24. Bromley ST, Flikkema E. Novel structures and energy spectra of hydroxylated (SiO2) 8-based clusters: Searching for the magic (SiO2) 8O2H3 cluster. J Chem Phys. 2005; 122(11): 114303. PMID: 15836211 DOI: 10.1063/1.1861889 [PubMed]

25. Bromley ST. Thermodynamic stability of discrete fully coordinated SiO2 spherical and elongated nanocages. Nano Letters. 2004; 4(8): 1427-32.

26. Zwijnenburg MA, Bromley ST, Jansen JC, Maschmeyer T. Toward understanding extra-large-pore zeolite energetics and topology: A polyhedral approach. Chemistry of Materials. 2004; 16(1): 12-20.

27. Pan W, Zhong W, Zhang D, Liu C. Theoretical study of the reactions of 2-chlorophenol over the dehydrated and hydroxylated silica clusters. J Phys Chem A. 2012; 116(1): 430-6. PMID: 22145640 DOI: 10.1021/jp208571d [PubMed]

28. Hoang VV. Molecular dynamics simulation of amorphous SiO2 nanoparticles. J Phys Chem B. 2007; 111(44): 12649-56. PMID: 17944505 DOI: 10.1021/jp074237u [PubMed]

29. Alderman SL, Dellinger B. FTIR investigation of 2-chlorophenol chemisorption on a silica surface from 200 to 500C. J Phys Chem A. 2005; 109(34): 7725-31. PMID: 16834148 DOI: 10.1021/jp051071t [PubMed]

30. Giannozzi P, Baroni S, Bonini N, Calandra M, Car R, Cavazzoni C, et al. QUANTUM ESPRESSO: A modular and open-source software project for quantum simulations of materials. Journal of Physics: Condensed Matter. 2009; 21(39): 395502.

31. Perdew JP, Burke K, Ernzerhof M. Generalized gradient approximation made simple. Phys Rev Lett. 1996; 77(18): 3865-8. PMID: 10062328 DOI: 10.1103/PhysRevLett.77.3865 [PubMed]

32. Monkhorst HJ, Pack JD. Special points for Brillouin-zone integrations. Physical Review B. 1976; 13(12): 5188.

33. Hourahine B, Aradi B, Blum V, Bonafé F, Buccheri A, Camacho C, et al. DFTB+, a software package for efficient approximate density functional theory based atomistic simulations. J Chem Phys. 2020; 152(12): 124101. PMID: 32241125 DOI: 10.1063/1.5143190 [PubMed]

34. Song J, Choi M. Stability of elongated and compact types of structures in SiO2 nanoparticles. Physical Review B. 2002; 65(24): 241302.

35. Gajewicz A, Puzyn T, Rasulev B, Leszczynska D, Leszczynski J. Metal oxide nanoparticles: Size-dependence of quantum-mechanical properties. Nanoscience & Nanotechnology Asia. 2011; 1(1): 53-8.

36. Gritsenko VA, Novikov YN, Shaposhnikov AV, Morokov YN. Numerical simulation of intrinsic defects in SiO2 and Si3N4. Semiconductors. 2001; 35(9): 997-1005.

37. Yadav AR, Sriram R, Carter JA, Miller BL. Comparative study of solution–phase and vapor–phase deposition of aminosilanes on silicon dioxide surfaces. Mater Sci Eng C Mater Biol Appl. 2014; 35: 283-90. PMID: 24411379 DOI: 10.1016/j.msec.2013.11.017 [PubMed]

38. Lu HT. Synthesis and characterization of amino-functionalized silica nanoparticles. Colloid Journal. 2013; 75(3): 311-8.